



Sub-band based Adaptive IIR Algorithm with Biquad Filter Stability Constraints for Feedforward Hear-Through Equalization

Rishabh Gupta¹, M L N S Karthik¹, Chelamkuri Omsrinath¹

¹Samsung Research Institute, Bangalore, India

rishabh.g@samsung.com, mk.srinivas@samsung.com, c.omsrinath@samsung.com

Abstract

Hear through (HT) filter is designed to provide a listening experience similar to open ear listening. The key challenge in the design of the HT filter is to ensure low processing delay to closely match the open ear response. Existing adaptive HT approaches such as adaptive finite impulse response (FIR) and neural network-based approaches can lead to higher processing delays. This paper proposes a sub-band based infinite impulse response (IIR) adaptive feedforward equalization method to improve the HT and convergence performance for sound sources incident from different directions. To ensure IIR filter stability, we propose inclusion of stability constraint based on least mean square fourth criterion. The proposed method improves performance over existing methods up to 13 dB for simulated outdoor and indoor scenarios, while maintaining stability and similar complexity as existing adaptive IIR and FIR techniques in simulated complex indoor and outdoor real-world acoustic environments.

Index Terms: Adaptive IIR filtering, Hear-through, Sub-band approach, feedforward systems

1. Introduction

The advancements in the audio technology have led to development of smart hearing assistive devices like hearing aids, headphones and ear buds. These devices provide highly immersive music playback, active noise control (ANC) and transparent mode in the hearing devices enhancing the comfort and situational awareness of the users [1-6]. While using earbuds or headphones, the external sounds are usually attenuated due to physical design of the earbuds [7, 8]. The main aim of transparency mode is to ensure that user has a listening experience similar to the open ear. This ensures the users can listen to different important external sounds like horns, conversations and emergency sirens etc. [5, 9]. The basic design of Hear-through (HT) system typically utilizes a reference microphone to capture the external signal, loudspeaker to play the pseudo-ambient signal and the error microphone to measure the signal near the ear drum. The signal captured from the reference microphone is processed by the HT filter and is played back through the loud speaker. This loud speaker signal is then combined with the passive isolated signal to generate the estimated ambient sound at the eardrum of the user [11].

Previous studies have mainly utilized FIR or IIR based fixed-filters for HT processing. Ramo and Valimiki developed an HT equalization (EQ) filter derived using the all-pass principle and analyzed the comb filtering effects [12, 13]. Zhaung et al. evaluated a frequency domain-based implementation of HT EQ filter using similar constraints as

ANC system design [14]. Some recent studies have also proposed adaptive FIR filters for improving acoustic transparency [9,15,16]. Ranjan and Gan evaluated the acoustic isolation caused by the open-back headphone devices and proposed EQ filtering using the adaptive FIR-based FxNLMS algorithms [9]. Patel et al. proposed a super directive beamformer using multi-reference feedforward control-based technique where the beampattern is steered towards the direction of ambient sound source [15]. Huang et.al. developed a Least Mean Square (LMS) based adaptive FIR filter combined with shaping filter for HT in insert type headphones [16]. Some studies have also explored combining Neural Network (NN) and dimensionality reduction techniques with FIR/IIR filtering to improve performance. In previous work, we proposed a parametric HT equalization based on shallow neural networks to compute direction of arrival for ambient sound and corresponding HT equalization filter selected from a database of pre-computed directional HT filters [25]. Jin et al. developed an individualized HT fixed FIR filter using the Principle Component Analysis (PCA) method to estimate the sound pressure at eardrum [18].

While the fixed-filter approaches utilized in past studies can lead to reduced computational complexity, they suffer from poor performance in dynamic real-world scenarios, such as stationary or moving sound sources from multiple directions, diffused sounds etc. Most of the previous adaptive filtering approaches utilize FIR filters, which provide enhanced stability and linear-phase characteristic desired for ambient filtering. However, the increased computational complexity can lead to additional processing delays and comb-filtering effects. The use of the IIR filters is more preferable as it can achieve similar performance to FIR filters with comparatively lower filter orders [19]. In this study, we propose a sub-band based adaptive IIR filter method for modelling the feedforward paths for ambient filters. Additionally, an all-pass biquad filter is cascaded to each adaptive IIR filter to compensate for additional phase and group delay caused during IIR filter weight stacking process during the adaptation. Furthermore, a novel constraint based on the combination of the stability triangle and least mean square fourth order update equation in terms of biquad coefficients is proposed. The proposed approach evaluated on different signals such as tonal, bandlimited white noise and complex signals simulating the real-world dynamic indoor and outdoor acoustic scenarios demonstrated superior performance compared to state-of-the art (SOTA) methods.

2. Proposed Approach

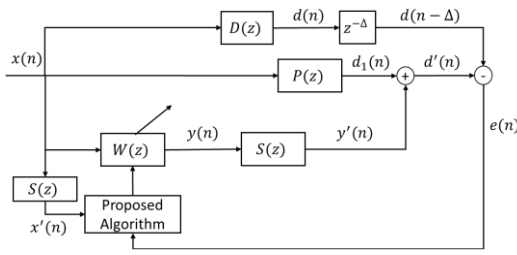


Figure 1: Hear-through filtering system

Figure 1 shows the generic block diagram of the hear-through equalization system. The ambient signal captured by the feedforward microphone is denoted by $x(n)$, acoustic path from the sound source(s) to the feedforward microphone is denoted by $P(z)$, and the reference open ear response is denoted as $D(z)$. $S(z)$ denotes the secondary path between the device loudspeaker and the eardrum, whereas the ambient filter is denoted as $W(z)$.

To ensure causality, a delay Δ is introduced in open ear response path to model for the total processing delay for the HT system. The so-called pseudo ambient signal $d'(n)$ received at the user's eardrum is denoted as

$$d'(n) = d_1(n) + y'(n) \quad (1)$$

where $d_1(n)$ denotes the leaked real signal and $y'(n)$ denotes the ambient signal played back through the device loudspeakers. To achieve acoustic transparency using the ambient filter $W(z)$, we need to minimize the error signal $e(n)$ as per mean square error criterion

$$e(n) = d(n - \Delta) - d'(n) \quad (2)$$

Using Z-transform in frequency domain, the optimal ambient filter $W^o(z)$ can be represented as

$$W^o(z) = \frac{D(z)z^{-\Delta} - P(z)}{S(z)} \quad (3)$$

Since $S(z)$ is non-minimum phase filter, the direct inversion can lead to a non-causal $W^o(z)$ filter. Hence, we propose to utilize a sub-band based adaptive approach for computing the ambient filter as shown in Fig. 2. The ambient signal $x(n)$ and error signal $e(n)$ are decomposed into P sub-bands using a decimation filter-bank is represented as $A(z)$ with decimation factor p . Each decimation filter $a_p(n)$ can be represented as

$$a_p(n) = a(n)e^{j2\pi pn/P} \quad (4)$$

The sub-band signals for ambient and error signals are used for adaptation of the corresponding biquad filter coefficients using the following update equation as per the least mean square fourth (LMS/F) moment criterion

$$w_p(n + P) = w_p(n) + \mu f(e_p(n))x'_p(n) \quad (5)$$

Where, $f(e_p(n)) = \frac{e_p^3(n)}{e_p^2(n) + \gamma}$, $e_p(n)$ is the error signal of each sub-band, step size is indicated as μ , and γ indicates threshold value [21]. The numerator coefficients of the biquad filter can be updated as

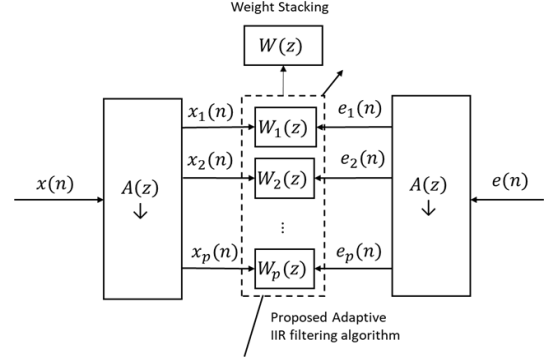


Figure 2: Adaptive IIR filtering algorithm with delay-less sub-band modelling

$$b_p(n + P) = b_p(n) + \mu f(e_p(n))x'_p(n) \quad (6)$$

The least mean square/forth (LMS/F) criterion is used since it has been shown in previous studies to lead to fast convergence and lower steady state error compared to other traditional LMS approaches [21]. The generic optimization function for each sub-band based on LMS/F can be represented as

$$\min_{W_p} e_p^2(n) - \gamma \ln(e_p^2(n) + \gamma) \quad (7)$$

However, an unconstrained LMS/F formulation can lead to IIR filter instability. In next section, we propose constraints for above optimization problem to ensure stability of IIR filters and present theoretical and empirical analysis for the proposed approach.

2.1 Deriving constraints to ensure stability of IIR filters

IIR filters can become unstable if poles lie outside the unit circle. The traditional method for utilizing an all-pass filter involves mirroring the unstable poles and placing it in cascade with minimum-phase filter. However, it leads to additional complexity and can result in undesired modifications to the overall phase of the HT filter. To ensure stability, we utilize the stability criterion for biquad filters utilized in previous studies, i.e., all poles must lie within the stability triangle [19]. To avoid quasi-stable conditions, we use a stricter stability criterion given as

$$a_{0,p}(n) = 1, |a_{2,p}(n)| < 1 \text{ and } |a_{1,p}(n)| < 1 + a_{2,p}(n) \quad (8)$$

Where, $a_{0,p}(n)$, $a_{1,p}(n)$ and $a_{2,p}(n)$ are the coefficients for the biquad IIR filter corresponding to the filter poles. Using the above criterion, the optimization function can be represented as

$$g(a_{1,p}(n), a_{2,p}(n)) = (|a_{1,p}(n)| - 1 - a_{2,p}(n)) + \text{sign}(a_{2,p}(n)) (|a_{2,p}(n)| - 1) \quad (9)$$

The resulting filter design problem is represented as a non-linear optimization function with linear constraints

$$\begin{aligned} \min_{W_p} \{ & e_p^2(n) - \gamma \ln(e_p^2(n) + \gamma) + \\ & g(a_{1,p}(n), a_{2,p}(n)) \} \\ \text{w.r.t } & \|a_p(n + 1) - a_p(n)\|_2^2 \leq \epsilon \end{aligned} \quad (10)$$

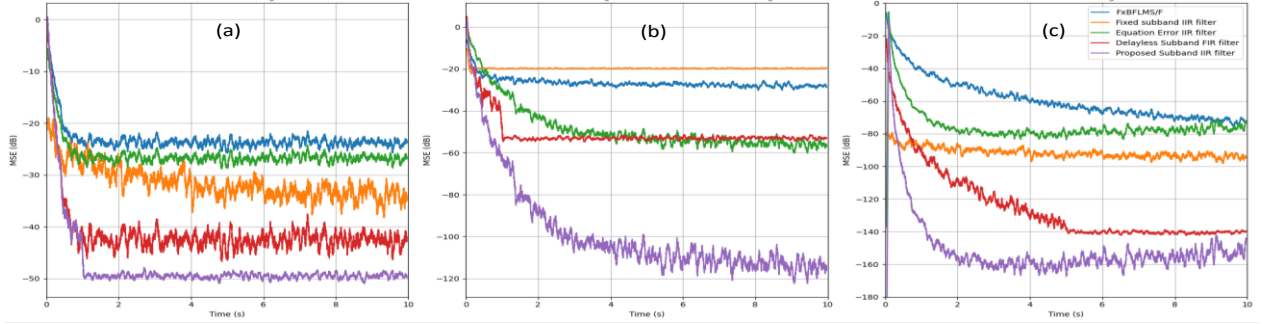


Fig. 3. MSE performance comparison for proposed vs state-of-the-art algorithms for different signals: (a) Multi-tone (500 Hz-2500 Hz); (b) Multi-tone (2kHz-3 kHz) with bandlimited white noise (5kHz-6 kHz range); (c) Broadband White noise (60 Hz to 8 kHz)

Using Lagrange's method, we can rewrite the above optimization function as

$$J(n) = e_p^2(n) - \gamma \ln(e_p^2(n) + \gamma) + g(a_{1,p}(n), a_{2,p}(n)) + \tau(\|a_p(n+1) - a_p(n)\|_2^2 - \epsilon) \quad (11)$$

On solving the above equation, we can obtain the update equation in terms of filter coefficients as

$$a_{1,p}(n+1) = a_{1,p}(n) - \frac{\epsilon [f(e_p(n))y_p'(n-1) + \text{sign}(a_{1,p}(n))]}{\|f(e_p(n))(y_p'(n-1) + y_p'((n-2))) + \text{sign}(a_{1,p}(n))\|_2} \quad (12)$$

$$a_{2,p}(n+1) = a_{2,p}(n) - \frac{\epsilon [f(e_p(n))y_p'((n-2))]}{\|f(e_p(n))(y_p'(n-1) + y_p'((n-2))) + 1 * \text{sign}(a_{1,p}(n))\|} \quad (13)$$

The above constraints ensure stability for each biquad filter corresponding to particular sub-band, thus ensuring overall filter stability. The obtained IIR filters are cascaded with the all-pass filters and weight stacking to compensate for the group delay and phase delay modification of the overall system [24]. For p^{th} sub-band filter, ϵ parameter is estimated using the approximation for convergence speed derived in [20] as

$$\frac{e_p^2(n)}{e_p^2(n+1)} \approx (1 - \epsilon \lambda_k)^{-2} \quad (14)$$

where λ_k is the eigenvalue associated with update of the error signal. If ϵ is assigned large values, the LMS/F algorithm may diverge. However, if $\epsilon \lambda_k \ll 1$, convergence rate will be very slow, leading to higher steady state error. Hence, ϵ must be fine-tuned to achieve desired performance and convergence speed.

3. Experiments and Results

To evaluate the performance of the proposed approach, we carry out the simulation experiments at the sampling frequency of 16 kHz. We evaluated the performance of the proposed algorithms compared to SOTA adaptive FIR and IIR algorithms such as Filtered-x Block based Least Mean Square fourth order

(FxBLMS/F) [21], equation error-based adaptive IIR [22], delayless sub-band based FIR filter [23]. We also compared the performance of proposed algorithm with sub-band based fixed-filter approaches.

3.1 Different Test signals - Single Sound Source Direction

To benchmark the performance of proposed adaptive IIR filter with different signal types, we utilized three stimuli with different frequency contents convolved with feedforward primary path for single source direction (0° elevation and 0° azimuth). For evaluating performance in different frequency regions, we utilized multi-tone and bandlimited white noise signals, whereas white noise signal was used to evaluate the broadband performance. The multi-tone signal consisted of sine tones at intervals of 500 Hz, starting from frequency of 500 Hz up to 2500 Hz to evaluate performance in regions most sensitive to tonal signals around 1kHz to 2 kHz. For narrowband signal evaluation, we utilized a combination of the multi-tone sinusoidal signals in 2 kHz to 3 kHz range together with the bandlimited white noise signal with bandwidth 5 kHz to 6 kHz. For evaluating performance with broadband signals, we utilized a white noise signal with frequency content in 60 Hz to 8 kHz range. The performance of proposed adaptive algorithms compared to the SOTA adaptive algorithms is shown in Fig. 3 for the three test signals. As seen from the graph, the proposed sub-band IIR filter has lowest steady-state mean square error (SS-MSE) of -50 dB or lower compared to the state-of-the-art fixed and adaptive algorithms for all the three test stimuli. The proposed approach shows improved performance over the delay-less sub-band FIR filtering techniques, which performs best among the SOTA methods. The proposed sub-band IIR filter is derived considering the stability constraints of the IIR filter and a fixed secondary path. For multi-tone and white noise signals, though the proposed algorithm performed best in terms of SS-MSE, the convergence time was longer compared to other SOTA algorithms. This could be due to multiple reasons, such as slower convergence in some sub-bands compared to others or selection of appropriate parameters, namely step size, and threshold parameters. The convergence performance of the existing algorithms such as delay-less sub-band FIR and equation error IIR was similar to the proposed algorithm in some cases.

3.2 Simulation of Dynamic Real Scenarios – Indoor and Outdoor Environments with multiple source directions

An outdoor environment is simulated for left ear with all sound sources located at 0° elevation, where user is listening to a sound of vehicle engine which is moving with constant speed of 15 km/hour with direction of arrival (DoA) (0° to 120°)

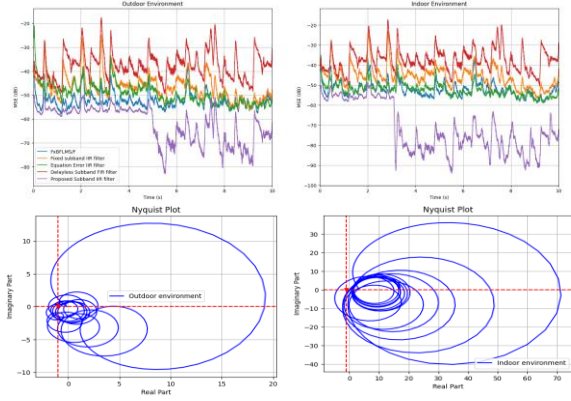


Fig. 4: MSE Performance Benchmarking for simulated environments (top) and stability analysis of proposed algorithm (Bottom); Simulated indoor environments (left), Simulated outdoor environment (right)

azimuth), experiencing a diffuse airplane signal with DoA of 5° resolution, a speech of person standing at fixed position with DoA of 75° azimuth and music played from two directions, 45° and 135° azimuth respectively. For simulating a complex indoor environment with all sound sources located at 0° elevation, the user is assumed to be sitting in a conference room with announcement coming from loudspeaker across room at DoA of 45° azimuth, a person moving across the room and talking from DoA of 0° to 120° azimuth, a cell phone ring tone and drilling sound coming from the outside the room at DoA of 60° and 120° , respectively. As observed from MSE plots in Fig. 4, proposed technique is able to track the changes in the sound sources with lower MSE compared to other state-of-the-art adaptive FIR algorithms, sub-band FIR algorithm and fixed IIR filters for both the indoor and outdoor cases. The average MSE of the proposed approach is lower by about 13 dB and 21 dB respectively for simulated outdoor and indoor environments

Table 1: Computational Complexity for Adaptive Algorithms

Algorithm	Computation Formula	MAC
FxBLMS/F (FIR)	$4L + 2N + 5$	645
Delayless Sub-band (FIR)	$8(\log_2 P) + (1 + \frac{2}{P})(\frac{16L+2N}{P}) + \frac{8L}{P} \left[\left(2 + \frac{4}{P}\right) \log_2 \frac{4N}{P} + \log_2 L \right]$	2220
Equation Error (IIR)	$4B + 4A + 6N - 1$	619
Proposed Adaptive Sub-band IIR filter	$P \left\{ P \log_2 P + \left(1 + \frac{2}{P}\right) \left[\frac{16L_a + 16L_b + N + 2}{P} + \frac{16L_a + 16L_b}{P} \left[\left(2 + \frac{4}{P}\right) \log_2 \frac{4(L_a + L_b)}{P} + \log_2(L_a + L_b) \right] \right] \right\}$	704

$$N = 64, L = 128, P = 8, B = 30, A = 29, L_a = 3, L_b = 2$$

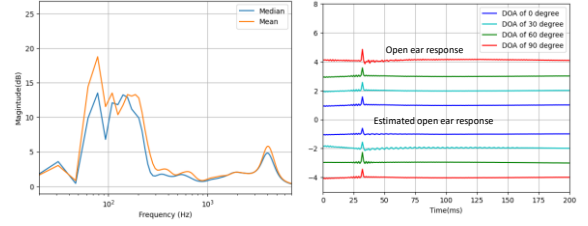


Fig. 5: Mean and Median Spectral error (Left), Measured and Estimated open ear impulse response at different source directions (Right)

compared to that of best performing SOTA algorithm. Further, Fig. 4 also shows the Nyquist plot for the proposed method in both indoor and outdoor scenarios with positive numbers of encirclements around the point $(-1, 0)$. The gain margin and the phase margin of the both outdoor and indoor environments is 10.48 dB, 310.85° and 9.53 dB, 270.58° respectively, demonstrating that the proposed IIR filter is stable for complex dynamic scenarios. Fig. 5 shows the spectral error and impulse responses of the open ear and estimated open ear signals. It is observed that proposed HT filter has low spectral error between the frequency range of 200 Hz to 6 kHz and higher spectral error at frequencies below 200 Hz. Additionally, lesser delay is also observed between estimated and measured open ear responses with proposed approach.

3.3 Computational Complexity Analysis

The computational complexity of the proposed adaptive IIR approach compared to state-of-the-art adaptive algorithms in terms of the number of MAC operations (multiply accumulate and add) is shown in the Table I. In Table 1, L denotes the length of FIR filter, N denotes the length of the estimated secondary path, whereas L_b and L_a denotes the length of coefficients for IIR filters respectively, and P denotes number of sub-bands. For the MAC computation shown in Table 1, the MAC operations include the total computation related to the feedforward ambient filter, namely computation of weights as per the update equation, convolution of the computed filter weights with the input signal, filtering operation through the secondary path (assumed as fixed path in this paper), and estimation of the error signal. As shown in the table 1, the proposed adaptive sub-band based IIR filter has the similar complexity in terms of MAC operations as the SOTA methods.

4. Conclusions

In this paper, a sub-band IIR adaptive HT EQ filter using the FxLMS/F combined with biquad stability constraint has been developed to improve performance for feedforward ambient filter control. The proposed sub-band adaptive IIR technique achieved superior HT performance for tonal, bandlimited and broadband white noise signals over existing state-of-the-art fixed IIR and adaptive IIR and FIR techniques in terms of mean square error. The proposed algorithm was evaluated on simulated complex real-world indoor and outdoor scenarios, where the proposed algorithm showed average performance improvements of 13 and 21 dB respectively over existing models, while maintaining stability in challenging dynamic scenarios. Future works can focus on hardware implementation of proposed sub-band adaptive algorithm for real-time evaluation.

5. References

- [1] "Hearable devices—Global market trajectory & analytics", Apr. 2021.
- [2] "Earphones and headphones market—Global outlook and forecast 2021-2026", Apr. 2021.
- [3] M. C. Killion, "Myths that discourage improvements in hearing aid design," *Hearing Review*, vol. 11, no. 4, pp. 32–70, 2004.
- [4] R. Sockalingam, J. Beilin, and D. L. Beck, "Sound quality considerations of hearing instruments," *Hearing Review*, vol. 16, no. 9, pp. 22–28, 2009.
- [5] V. Valimaki, A. Franck, J. Ramo, H. Gamper and L. Savioja, "Assisted listening using a headset: Enhancing audio perception in real augmented and virtual environments," *IEEE Signal Process. Mag.*, vol. 32, no. 2, pp. 92-99, Mar. 2015.
- [6] W.-S. Gan, J. He, R. Ranjan and R. Gupta, "Natural and augmented listening for VR and AR/MR," *Proc. ICASSP Tutorial*, Apr. 2018.
- [7] C.-Y. Chang, A. Siswanto, C.-Y. Ho, T.-K. Yeh, Y.-R. Chen and S. M. Kuo, "Listening in a noisy environment: Integration of active noise control in audio products," *IEEE Consum. Electron. Mag.*, vol. 5, no. 4, pp. 34-43, Oct. 2016.
- [8] M. T. Khan and R. A. Shaik, "High-performance hardware design of block LMS adaptive noise canceller for in-ear headphones," *IEEE Consum. Electron. Mag.*, vol. 9, no. 3, pp. 105-113, May 2020.
- [9] R. Ranjan and W.-S. Gan, "Natural listening over headphones in augmented reality using adaptive filtering techniques," *IEEE/ACM Trans. Audio Speech Language Process.*, vol. 23, no. 11, pp. 1988-2002, Nov. 2015.
- [10] S.-N. Yao, "Headphone-based immersive audio for virtual reality headsets," *IEEE Trans. Consum. Electron.*, vol. 63, no. 3, pp. 300-308, Aug. 2017.
- [11] R. Gupta, R. Ranjan, J. He, W.-S. Gan and S. Peksi, "Acoustic transparency in hearables for augmented reality audio: Hear-through techniques review and challenges," *Proc. AES Int. Conf. AVAR*, pp. 3-7, Aug. 2020.
- [12] J. Ramo and V. Valimaki, "An allpass hear-through headset," *Proc. 22nd Eur. Signal Process. Conf. (EUSIPCO)*, pp. 1123-1127, Sep. 2014.
- [13] J. Ramo and V. Valimaki, "Digital augmented reality audio headset," *J. Electr. Comput. Eng.*, vol. 2012, pp. 1-13, Oct. 2012.
- [14] Y. Zhuang and Y. Liu, "A constrained optimal hear-through filter design approach for earphones," *Proc. 50th Int. Congr. Expo. Noise Control Eng. (INTERNOISE)*, pp. 1329-1337, Aug. 2021.
- [15] V. Patel, J. Cheer and S. Fontana, "Design and implementation of an active noise control headphone with directional hear-through capability," *IEEE Trans. Consum. Electron.*, vol. 66, no. 1, pp. 32-40, Feb. 2020.
- [16] C. R. Huang, C. Y. Chang and S. M. Kuo, "Time-Shift Modeling-Based Hear-Through System for In-Ear Headphones," in *IEEE Transactions on Consumer Electronics*, vol. 68, no. 3, pp. 273-280, Aug. 2022, doi: 10.1109/TCE.2022.3190422.
- [17] Y. Zhuang and Y. Liu, "A constrained optimal hear-through filter design approach for earphones," *Proc. 50th Int. Congr. Expo. Noise Control Eng. (INTERNOISE)*, pp. 1329-1337, Aug. 2021.
- [18] W. Jin, T. Schoof and H. Schepker, "Individualized hear-through for acoustic transparency using PCA-based sound pressure estimation at the eardrum," *Proc. IEEE 47th Int. Conf. Acoust. Speech Signal Process. (ICASSP)*, pp. 341-345, May 2022.
- [19] F. Hilgemann, J. Fabry, and P. Jax. "Design of IIR filters for active noise control by constrained optimization," *2021 29th European Signal Processing Conference (EUSIPCO)*. IEEE, 2021.
- [20] M. R. Petraglia and D. B. Haddad "Mean-square error and stability analysis of a subband structure for the rapid identification of sparse impulse responses," *Digital Signal Processing*, Volume 22, Issue 6, 2012, pp. 1068-1072.
- [21] M. L. N. S. Karthik, S. Joel, and Nithin V. George. "FxLMS/F Based Tap Decomposed Adaptive Filter for Decentralized Active Noise Control System," *IEEE/ACM Transactions on Audio, Speech, and Language Processing* 32 (2024): 4691-4699.
- [22] C. Y. Ho, K. K. Shyu, C. Y. Chang, and S. M. Kuo. "Development of equation-error adaptive IIR-filter-based active noise control system," *Applied Acoustics*, 163, 107226 (2020).
- [23] S. Pradhan, X. Qiu and J. Ji. "A Variable Step Size Improved Multiband-Structured Subband Adaptive Feedback Cancellation Scheme for Hearing Aids," *2020 Asia-Pacific Signal and Information Processing Association Annual Summit and Conference (APSIPA ASC)*. IEEE, 2020.
- [24] L.C. Su, Y. D. Jou, & F.K. Chen, "An efficient least-squares design of IIR all-pass filter," In *TENCON 2009-2009 IEEE Region 10 Conference* (pp. 1-5). IEEE, 2009.
- [25] R. Gupta, R. Ranjan, J. He and W. S. Gan, "Parametric Hear through Equalization for Augmented Reality Audio," *ICASSP 2019 - 2019 IEEE International Conference on Acoustics, Speech and Signal Processing (ICASSP)*, Brighton, UK, 2019, pp. 1587-1591, doi: 10.1109/ICASSP.2019.8683657.